SOILS AND FOUNDATIONS Vol. 20, No. 1, Mar. 1980
Japanese Society of Soil Mechanics and Foundation Engineering

CYCLIC SIMPLE SHEAR TESTS ON SATURATED SAND IN MULTI-DIRECTIONAL LOADING

KENJI ISHIHARA* and FUMIO YAMAZAKI**

ABSTRACT

Several series of multi-directional undrained simple shear tests were performed on saturated sand specimens, using a simple shear test device incorporating two pnumatic cyclic loaders in two mutually perpendicular horizontal directions. The load patterns employed were rotational in one type of test where cyclic stresses with equal or different amplitudes in two directions were applied with a phase difference of 90 degree. In the second type of test, cyclic stresses with equal or different amplitudes in two directions were alternately applied with a phase difference of 360 degrees. The results of these tests have shown that the cyclic stress ratios causing 5% simple shear strain in the specimen under multi-directional loadings with two equal amplitudes were on an average 70% as much as the similarly defined cyclic stress ratio under uni-directional loading condition.

Key words: earthquake, liquefaction, repeated load, sand
IGC: D 6/D 7

INTRODUCTION

When a soil element in the level ground is shaken by motions due to upward propagation of shear wave during earthquakes, the major stresses imparted on the soil element would be erratic sequences of simple shear stresses in the horizontal plane involve changes not only in amplitude but also in direction. Because of difficulty in building a test apparatus permitting a simulation of such complex stress changes in the laboratory, most of the laboratory cyclic tests performed thus far were those in which stresses were reciprocated only in one direction. The first attempt to investigate a problem associated with this was made by Pyke, Seed and Chan (1975). They conducted several series of multi-directional shaking table tests in which a layer of dry sand in a small shaking table was mounted transversely on another large shaking table. It was discovered that settlements of the sand layer observed in the shaking in one direction only was less than the settlements measured during the multi-directional shaking. Based on these test results, Seed, Pyke and Martin (1978) calculated the resistance to liquefaction of the same sand that would have been obtained in a simple shear type stress condition if the sand had been saturated and subjected to uniform cyclic stresses executed in a gyratory manner. It was found that the resistance to liquefaction under 20 cycles of uniform loading under gyratory shear stress condition would be approximately 15% smaller than the liquefaction resistance that would be obtained in uni-directional loading. More recently, Casagrande and Rendon (1978) designed and constructed a simple shear test apparatus in which cyclic shear stresses could be applied in multi-directional loading conditions.

* Professor of Civil Engineering, University of Tokyo, Bunkyo-ku, Tokyo.
** Civil Engineer, Shimizu Construction Co., Chuo-ku, Tokyo.
Written discussions on this paper should be submitted before January 1, 1981.

In view of unknown factors yet to be investigated with respect to the sand behavior under multi-directional loading, an attempt was made to construct a simple shear test apparatus enabling the application of shear stresses in any desired manner in two mutually perpendicular directions. The following pages describe the design and operation of the apparatus and also present some test results obtained through the use of this apparatus.

DESCRIPTION OF THE SIMPLE SHEAR DEVICE

The apparatus used for this study consisted of three main components : two mutually perpendicular horizontal loading device, an assemblage for specimen placement, and an equipment for applying vertical load. A schematic illustration of the apparatus is given Fig. 1.

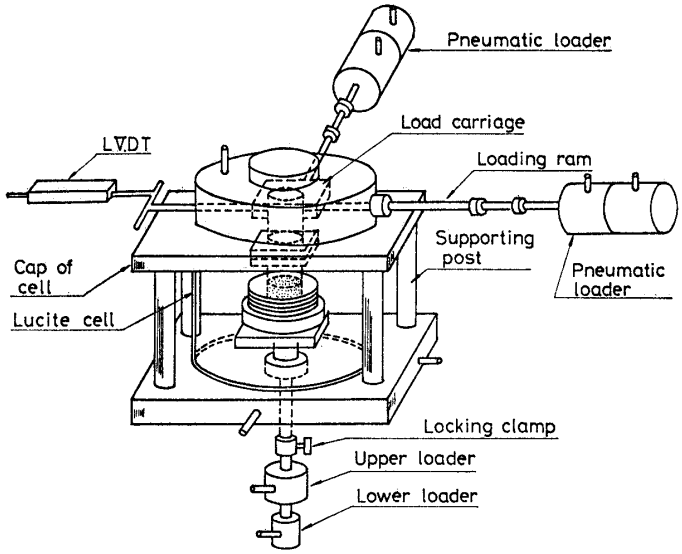

Fig. 1 Schematic illustration of the two-directional simple shear test apparatus

Horizontal Loading Unit

Two identical loading rams were arranged to apply cyclic force on the specimen in two mutually perpendicular horizontal directions. Each ram was capable of applying a maximum static load of 3 500 kN and cyclic load of 2 200 kN. Load was transmitted to the specimen by way of a specially designed carriage fitted to the top cap of the cell. The schematic plan of the load carriage is shown in Fig. 2. The carriage was designed to apply load to the specimen only along the thrust axis of its activating jack whilst, at the same time, permitting free horizontal movement perpendicular to this axis. This was achieved by the arrangement of a ball bearing system as shown in Fig. 2. The motion of the load carriage was restricted to a movement in the horizontal plane by guide ball bearings. Thus, it was possible to obtain independent operation of loadings in two mutually perpendicular directions without generating undesirable interaction between the two horizontal loading devices during cyclic loading tests. Each of the loading ram was connected to a pneumatic loader through a load cell which monitored the intensity of load trasmitted to the specimen. The load cells (U. S. Trans, INC, SG-type), placed inside the cell, had a maximum capacity of 2 270 kN. Linear variable differential transformer (Shinko, SG-type) having a maximum stroke of ± 20 mm were connected on the opposite side of the loading ram to horizontal rods as shown in Fig. 1 to monitor the horizontal displacement at the top of the specimen.

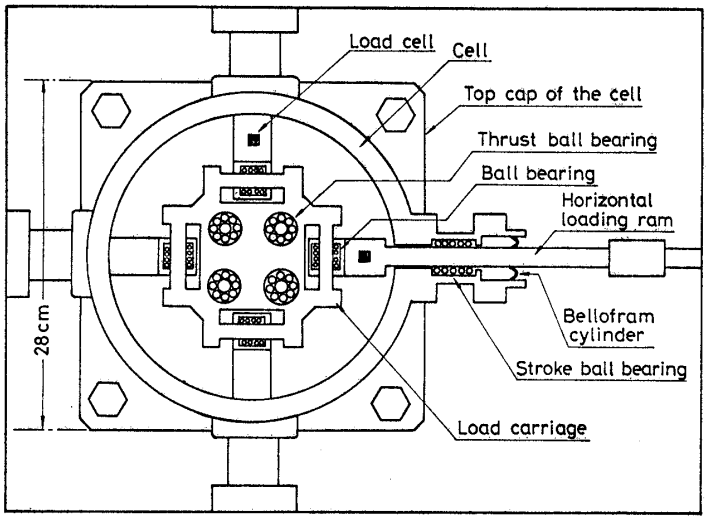

Fig. 2 Schematic plan picture of the load carriage

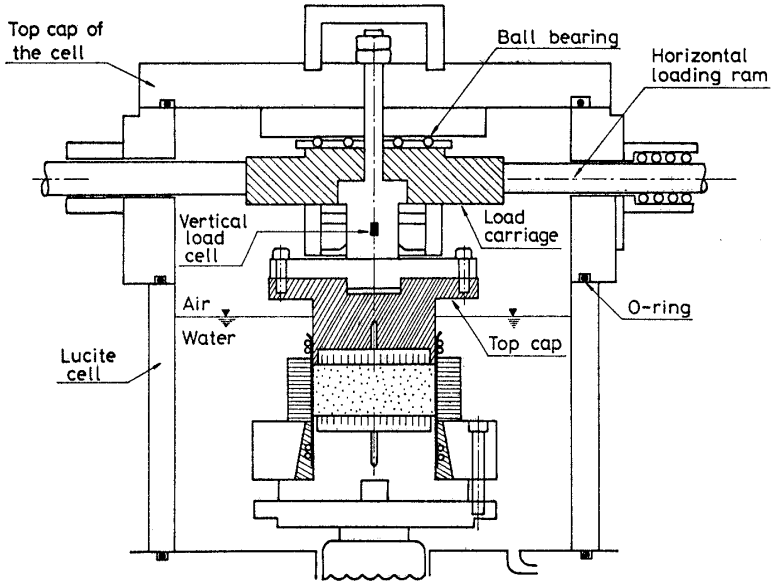

Fig. 3 Setup of the simple shear test apparatus

Vertical Loading Unit

Two independently operating pneumatic rams were installed below the test cell to apply loads vertically upwards. The upper cylindrical ram, having a maximum capacity of 4 910 kN, was installed to apply static vertical stress to the specimen during consolidation. It was also used to support the weight of the platform and any ancillary devices which might be placed on it. The lower ram (maximum capacity 2 220 kN) shown in Fig. 1 was designed to provide a force to counterbalance the vertical pressure produced in the cell due to the application of cell pressure. A mechanism to clamp the vertical loading rod in any desired position was provided just beneath the test cell. In order to monitor the vertical stress, if necessary, during cyclic loading test, a load cell (Seiken No. 123) with a maximum capacity of 3 000 kN was attached to the vertical shaft above the specimen cap inside the test cell.

Assemblage for Specimen Placement

The soil specimen was enclosed in a rubber membrane which was secured to the top cap

and the base plate by means of O-rings. The flank of the membrane-enclosed specimen was surrounded by a stack of teflon coated annular plates as shown in Fig. 3 to prevent lateral displacement during cyclic simple shear test. Drainage lines were provided both through the top cap and the base plate of the specimen. One of the drainage line was connected to the pressure transducer (Kyowa, PGM, 500 kN/m²) installed at the pedestal of the test cell. An ancillary device was provided to apply back pressure through the drainage lines. The top cap was rigidly connected to the unit of the load carriage so that the horizontal load was transferred with minimum rocking to the top surface of the specimen.

TEST MATERIAL AND SAMPLE PREPARATION

The sand used in the present investigation was obtained from the bed of the Fuji river, due west of Tokyo. Subangular in grain shape, it had a specific gravity of 2.728, a mean particle size of 0.40 mm and a uniformity coefficient of 3.16. The grain size distribution of the sand was as shown in Fig. 4. The maximum and minimum void ratios as measured by the procedure described elsewhere by Ishihara, Silver and Kitagawa (1978) were 1.032 and 0.481, respectively.

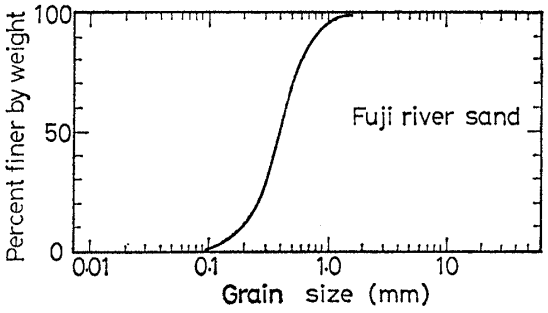

Fig. 4. Grain size characteristics of the sand used

When preparing a specimen in the simple shear divice as described above, a rubber membrane 0.025 mm thick was first fastened with O-rings to the base of the test cell as illustrated in Fig. 5. Then, a stack of teflon coated annular plates, each 1.0 mm thick, were placed outside the rubber membrane, together with the specially designed mold shown in Fig. 5. After rolling back the membrane over the top edge of the mold, suction was applied to hold the rubber membrane tight to the stack of annular plates. The mold was half filled with deaired water. Sand saturated with deaired water was then poured into the mold and sedimented under water. When the mold was approximately half full, the pedestal of the mold was tapped 5 times with a small wooden hammer. Pouring was then resumed until the mold was filled up to the desired height. The mold was tapped once again and the surface of the specimen was

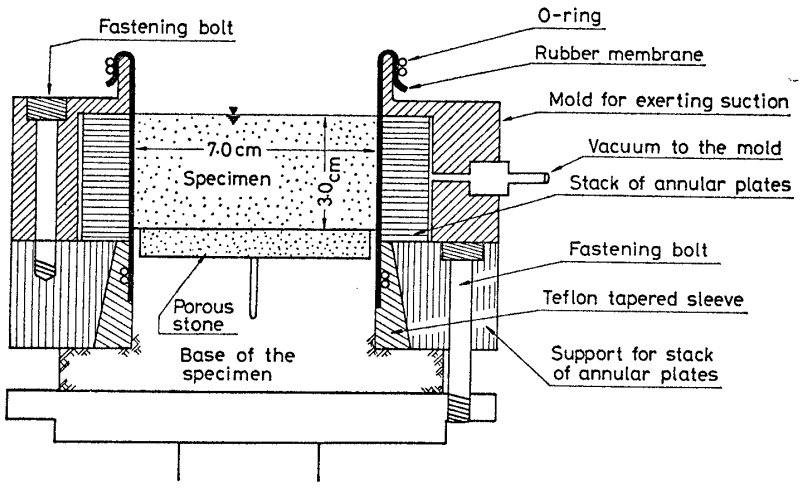

Fig. 5. Illustration for specimen preparation

smoothed off. A special holder was fabricated for the sample top cap, allowing it to be lowered gently on to the surface of the specimen. The top cap equipped with a saturated porous disk on its bottom surface was slowly lowered, while being supported by the cap holder, until it touched down the smoothed surface of the specimen. At this stage the suction applied to the inner space of mold was released. The top cap was then rigidly fixed temporarily to the holder, thereby preventing any vertical movement. The rubber membrane was rolled over and secured to the top cap with O-rings. A slight vacuum of 5 kN/m² was then applied to the pore water inside the specimen. While applying the vacuum the mold was dismantled. The height of the specimen was then measured by marking the vertical position of the top cap. The holder was removed and at this stage the top cap perched by itself on the specimen supported by vacuum. A transparent lucite cell was put in place and the cell cap was gently lowered onto the cell by means of a small crane. The cell cap was fixed by bolts to four vertical columns installed outside the cell. The base platform on which the specimen with the cap now rested was gently lifted by increasing the air pressure in the pneumatic ram located below the test cell. When the specimen top cap touched the plate beneath the vertical load cell, both were connected rigidly by means of four screws. Water was then introduced into the cell to a height a little above the level of the top of the specimen, leaving air in the upper portion of the cell. The cell pressure and vertical pressure were increased, while reducing the suction in the specimen, to achieve an isotropic consolidation with a small confining stress of 20 kN/m². Carbon dioxide (CO_2) was percolated through the specimen to ensure a satisfactory degree of saturation. Then, the vertical load was increased concurrently with the cell pressure to achieve a desired effective confining stress. A back pressure of 100 kN/m² was employed to achieve saturation with a B-value exceeding 0.95.

CYCLIC SIMPLE SHEAR TESTS

All cyclic simple shear tests were performed with an initial effective vertical stress of 200 kN/m². With respect to the lateral stress, there were three possible ways to control the cell pressures.

(i) The first option was to apply a cell pressure approximately equal to the lateral stress which would have been created in the specimen according to the appropriate K_0-condition. For instance, a cell pressure half the effective vertical stress would have been applied assuming the K_0-value to be 0.5. However, it has been shown by a previous study (Ishihara et al., 1978) that the liquefaction of sand occurs concurrently with an increase in lateral stress to produce an isotropic stress condition. Therefore, even if the cell pressure is kept always half the vertical stress, the lateral stress induced in the specimen tends to become greater than the cell pressure as the pore water pressure increases during cyclic loading. When the lateral stress in the specimen becomes larger than the cell pressure the rubber membrane would inflate at the unsupported section of the membrane on the top cap of the specimen as illustrated in Fig. 6. The inflation of the rubber membrane as above would be detrimental to the satisfactory operation of the simple shear device in which the volume of a specimen must be kept unchanged during cyclic load application.

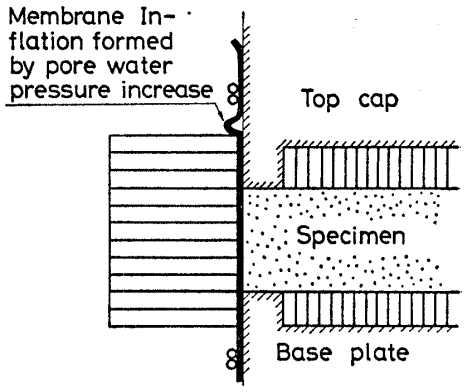

Fig. 6. Inflation of rubber membrane due to pore water pressure increase over the cell pressure.

(ii) The second option was to keep the cell pressure at zero. Some lateral stress would be

induced in the specimen due to the lateral constraint imposed by the stack of annular plates during application of the vertical stress. The amount of the lateral stress induced in this case would depend mainly on the coefficient of earth pressure at rest of the test material. However, during cyclic simple shear following the consolidation, the pore water pressure in the specimen increased well over the small pressure in the cell. Therefore, it is apparent that the membrane inflation as above can occur in a more exaggerated manner.

(iii) The third option was to apply a cell pressure equal to the initial effective vertical stress. In this case, the specimen would be brought initially to a state of isotropic consolidation and then subjected to cyclic simple shear. In this test, any undesirable membrane inflation, such as that described above, would be avoided, although the initial state of stress would be different from that encountered in the normal simple shear test condition. Despite these inconveniences, it appeared most appropriate and practical to employ a cell pressure equal to the vertical stress when the specimen was initially consolidated. Thus, a cell pressure of 300 kN/m^2 was used to achieve an isotropic consolidation in all the tests in this investigation.

In the equipment used in this study, it was possible to perform two kinds of simple shear test ; one in which the vertical stress was kept constant with free vertical displacement of the specimen being allowed during cyclic loading ; and the other in which vertical displacement was not permitted while the vertical stress was allowed to change during cyclic loading. After several trial tests, it was found that the type of test in which vertical displacement was allowed to take place gave lower resistance to liquefaction than the test with vertical confinement. It was hypothesized that the free vertical displacement produced an additional component of cyclic shear strain other than the cyclic simple shear, causing the specimen to become less resistant to liquefaction. For this reason, the locking clamp shown in Fig. 1 was employed to inhibit any vertical displacement during the application of cyclic simple shear in all the tests described in the following pages.

The simple shear device used in this study had a defect to produce rocking motions around the horizontal axis, and therefore when the vertical displacement was inhibited during shear, vertical stress was induced near the edge of the specimen. The non-uniformity of stress distribution within the specimen caused by the rocking motion was diffcult to evaluate at this stage of the test performance.

Because of the rocking motions, the horizontal displacement measured at the level of the horizontal load ram was approximately 0.06 cm greater than the displacement occurring at the top of the specimen. This means that the shear strain calculated using the measured displacement of the load ram was approximately 2% larger than the real shear strain induced in the specimen. The correction to this effect was made in the data processing.

Because of the friction generated in the carriage system, the horizontal load applied to the specimen's top was considered smaller than the load monitored by the load cell. To correct for this difference, water was encased in the rubber membrane and a small magnitude of force was measured during simple shear.

TEST SCHEME

A variety of shearing motions can be obtained by combining two horizontal components. Patterns of motion in a horizontal plane which are typical of those during earthquakes would at times be somewhat circular but would also include excursions in various directions. Two types of resultant motion were employed to reproduce this type of behavior in the simple shear test device.

Rotational Simple Shear Test

This type of test employed a resultant motion in the horizontal plane tracing circular or elliptic patterns as illustrated in Fig. 7. To produce the circular pattern, sinusoidal

simple shear motions in two mutually perpendicular directions were programmed to have equal amplitude. In the elliptic pattern, different amplitudes were employed to execute sinusoidal simple shear motion in two mutually perpendicular directions. In both cases, one component of motion was programmed to start one quarter of a cycle later than the other so that two motions were 90 degrees out of phase with each other. As an extreme case, one component was reduced to zero, thereby reverting to uni-directional simple shear. In the test, each component of motion was cycled with a frequency of 0.25 Hz.

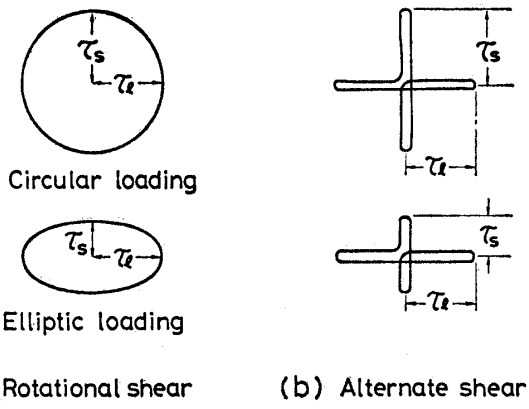

Fig. 7. Patterns of loading paths

Alternate Simple Shear Test

This type of test merely employed alternate excursions of sinusoidal simple shear motion in two mutually perpendicular directions. One component of motion was programmed to start one full cycle later than the other. Different amplitudes were also employed between the two components of cyclic simple shear. The pattern of the motion is illustrated in Fig. 7(b). In this test, each cycle was executed with a frequency of 0.25 Hz.

TEST RESULTS

Results from a uni-directional cyclic simple shear test are presented in Fig. 8. In this test, cyclic shear stress in only one direction (Y-direction) was applied to a specimen prepared with a relative density of 49%. The amplitude of cyclic stress in the Y-direction which will be denoted by τ_l (see Fig. 7) was 31.8 kN/m^2, while the amplitude in the X-direction, τ_s, was zero. Therefore, the cyclic stress ratio defined as the ratio between the amplitude, τ_l, and the initial effective vertical confining stress, σ'_v, was 0.159 in this particular test. It may be seen in Fig. 8 that the pore water pressure became equal to the initial confining pressure after 45 cycles, accompanied by a large shear strain, leading to liquefaction of the specimen. This is a behavior that is typically observed in most simple shear tests. Also shown in Fig. 8 are the negligibly small changes in shear stress and shear strain in the X-direction. These small changes were caused by an interaction in the mechanism of loading system, but its effect on the measured values may be disregarded. The large strain of approximately 2% recorded from the start of the cyclic test was caused by the rocking motion of the load-transmitting devices placed on top of the specimen. The result of the uni-directional simple shear test is summarized in Fig. 9.

Rotational Simple Shear Test

Typical test records for a rotational simple shear test are reproduced in Fig. 10. In this test, the cyclic stress ratio with respect to the Y-direction, τ_l/σ'_v, was 0.092 and the cyclic stress ratio with respect to the X-direction, τ_s/σ'_v, was 0.081. Therefore, the ratio between two cyclic shear stress amplitudes, τ_s/τ_l, was 0.88. It may be generally seen from Fig. 10 that the pore water pressure built up gradually as the shear stresses were cycled with shear strains increasing gradually. One aspect of the observed behavior deserving particular attention in the rotational simple shear test is the fact the pore water pressure stopped increasing when it became approximately 90% of the initial confining pressure even after the shear strains began to develop considerably. Thus, initial liquefaction in the

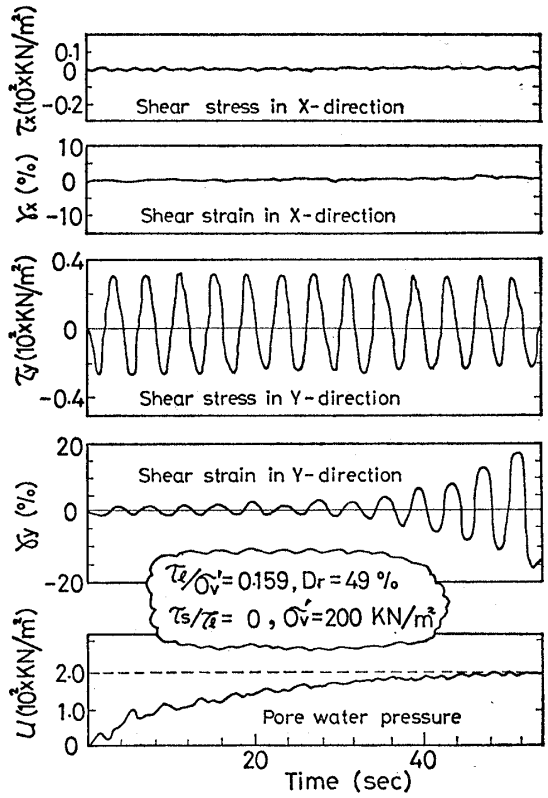

Fig. 8. Recorded time histories of cyclic stresses, cyclic strains and pore water pressures for a uni-directional simple shear test

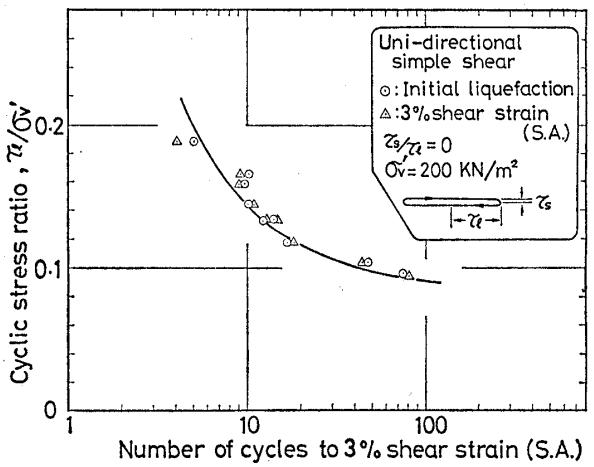

Fig. 9. Cyclic stress ratio versus number of cycles for uni-directional simple shear tests

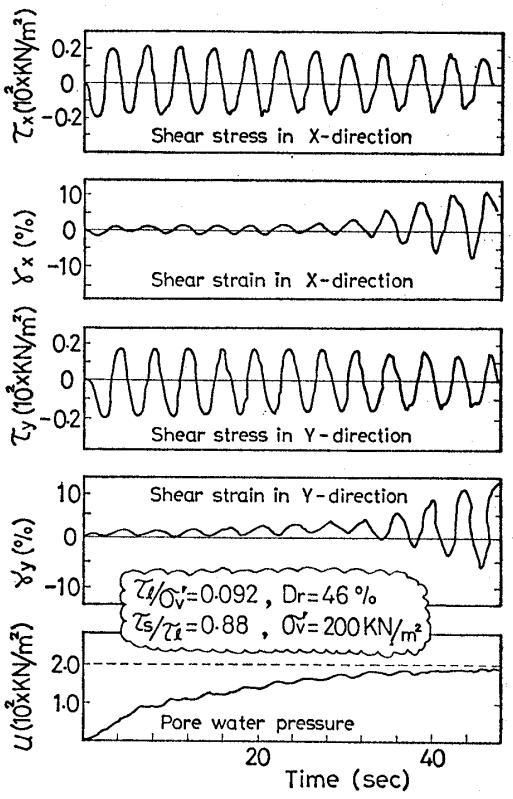

Fig. 10. Recorded time histories of cyclic stresses, cyclic strains and pore water pressures for a rotational simple shear test

sense that the pore water pressure becomes equal to the initial confining stress never occurred. The rotational simple shear may be deemed as consisting of an application of continuous change in the direction of simple shear superimposed on a simple shear initially applied to the specimen. Therefore, during rotational shearing, the sample is always kept deformed (in a simple shear manner due to the initially applied simple shear) to the range of strain on which the specimen tends to dilate. Consequently, the pore water pressure during rotational shear is inhibited from becoming equal to the initial confining stress. To provide evidence for the above reasoning, the simple shear stress was brought back to zero

in one test when the pore water pressure had become equal to 90% of the initial confining stress. It was then observed that the pore water pressure became exactly equal to the initial confining pressure immediately after the simple shear stress was released.

For the reason mentioned above, it was considered inadequate to define the specimen failure in the rotational simple shear in terms of the initial liquefaction criterion. A number of rotational shear tests performed in this study have indicated that the single amplitude cyclic strain was approximately 3% at the time the pore water pressure became equal to 90% of the initial effective confining pressure. Therefore, failure of specimens in rotational shear was defined as being the instance when the single amplitude cyclic shear strain had become equal to 3%. This failure criterion will be used throughout this paper.

The results of tests employing the rotational simple shear are presented in Fig. 11, where the cyclic stress ratios in terms of the Y-component causing 3% single amplitude shear strain are plotted versus the number of cycles. The number of cycles plotted here was the number counted only for repetition of load in the Y-component. Fig. 11 (a) shows the results of tests in which the rotational shear was nearly circular with the ratio between the shorter and longer axes ranging between 0.8 and 1.0. Fig. 11 (b) is a similar result for tests with the cyclic stress amplitude ratio, $\tau_s/\tau_l = 0.6$ to 0.8. The test results for cases where the values of the cyclic stress have lesser amplitude ratio than the previous two are presented in Fig. 11(c) and 11(d). The above test results are summarized in Fig. 12, to-

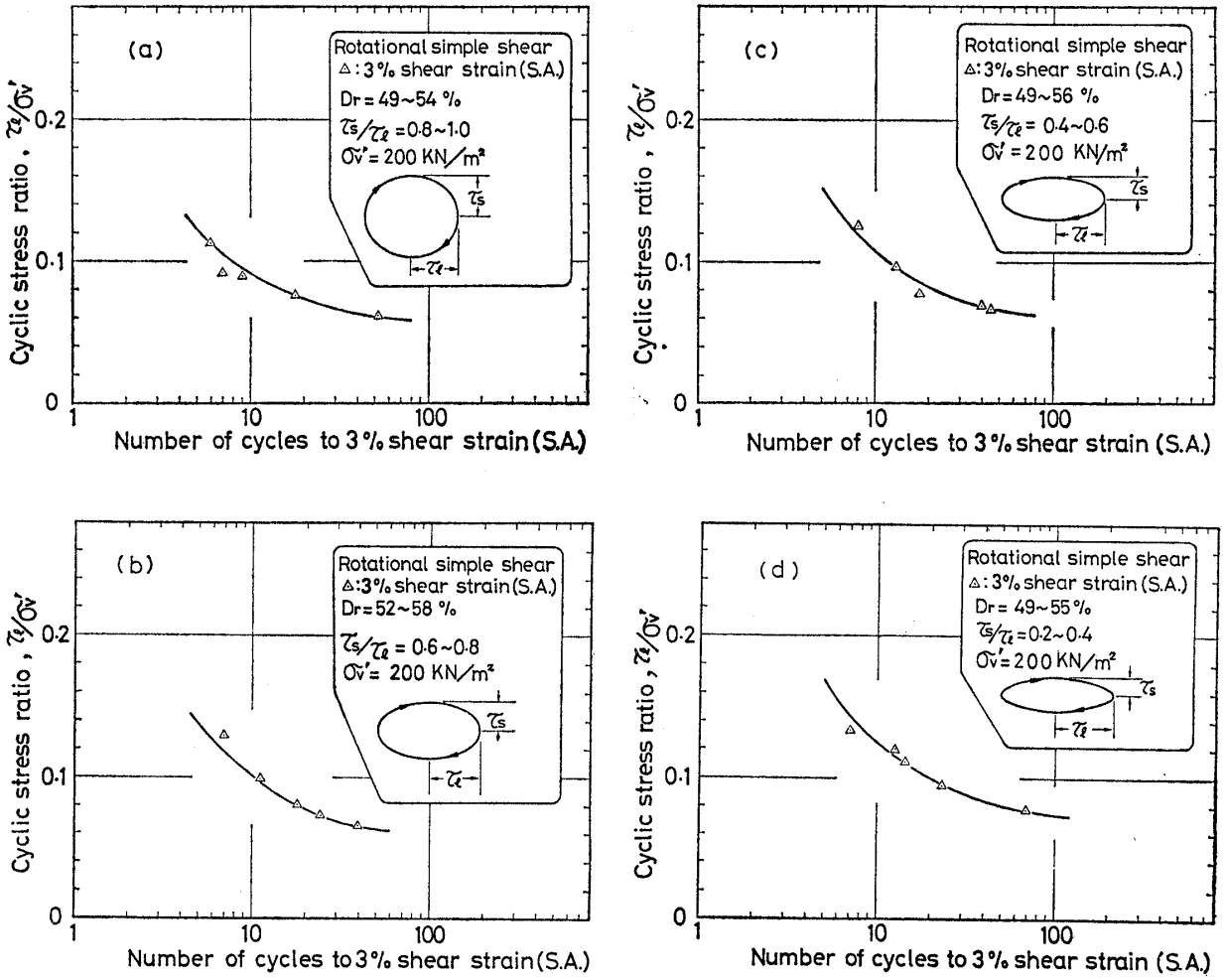

Fig. 11. Cyclic stress ratio versus number of cycles for rotational simple shear tests

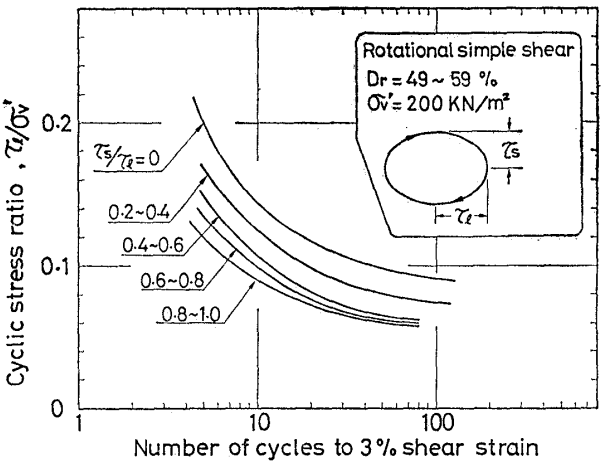

Fig. 12. Summary of the rotational simple shear tests

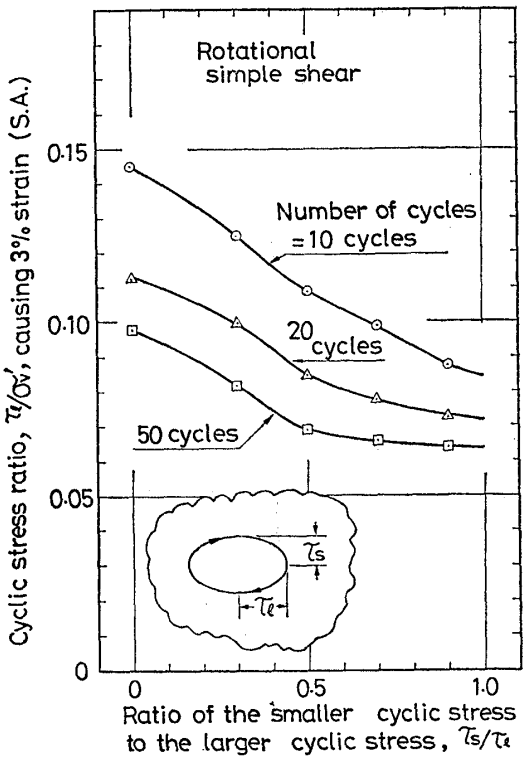

Fig. 13. Cyclic stress ratio versus cyclic stress amplitude ratio between two directions

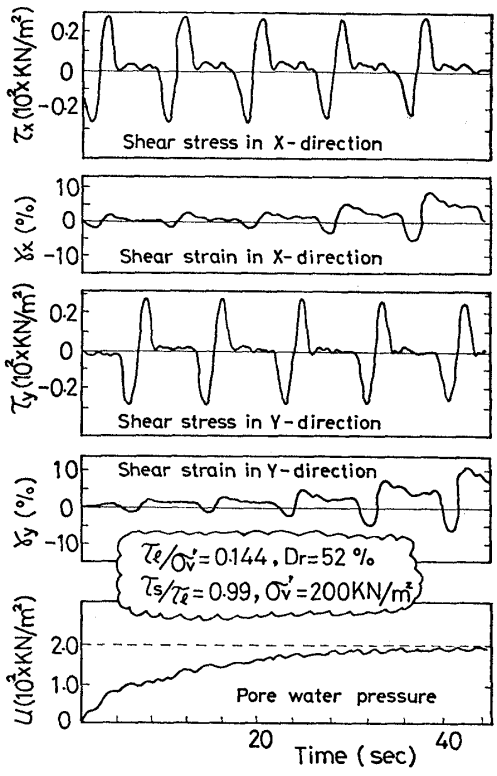

Fig. 14. Recorded time histories of cyclic stress, cyclic strains and pore water pressure for an alternate simple shear test

gether with the result from the uni-directional simple shear test result shown in Fig. 9. It may be seen in Fig. 12 that the cyclic stress ratio in one direction necessary to cause 3% single amplitude shear strain in the same direction decreased as the cyclic stress amplitude in the other direction perpendicular to it was increased. In other words, the more circular the stress path in the plane of simple shear becomes, the less resistant the specimen becomes to induce 3% single amplitude strain for a given number of cyclic stress applications. In order to visualize the effect that the cyclic stress in the X-direction has on the cyclic strength in the Y-direction, the cyclic stress ratio values causing 3% single amplitude shear strain in the Y-direction in 10, 20 and 50 cycles were read off from Fig. 12 and replotted in Fig. 13 versus the cyclic stress amplitude ratio, τ_s/τ_l. It may be seen in Fig. 13 that the

cyclic stress ratio causing failure with respect to the direction of larger shear stress application decreases rather sharply as the cyclic stress amplitude ratio increases from zero to 0.5, but more gradually as it further increases from 0.5 to 1.0.

Alternate Simple Shear Test

Typical test records for the alternate simple shear tests in which the cyclic stress amplitudes in X- and Y-directions were almost the same are reproduced in Fig. 14. It may be seen that, unlike in the case of the rotational shear as described above, the pore water pressure became exactly equal to the initial confining pressure. This indicates that the initial liquefation could occur in the alternate simple shear test. In this type of test, the simple shear stress is reduced to zero once in half a cycle and, hence, the initial liquefaction could occur. However, in order to maintain a consistency with the rotational shear test in representing the results, the 3% single amplitude criterion will again be adopted in the case of the alternate shear tests. The alternate shear test results are presented in Fig. 15 in terms of the cyclic stress ratio versus the number of cycles with respect to the direction of the larger cyclic stress amplitude. Fig. 15(a) shows the results of tests in which the cyclic stress amplitude ratio, τ_s/τ_l, ranged between 0.8 and 1.0. The subsequent figures in Fig. 15 show the results of similar test but smaller values of τ_s/τ_l. These test results are summarized in Fig. 16. Also shown in Fig. 16 for purposes of comparison is the result of uni-directional simple shear test quoted from Fig. 9. It is apparent that the effect of increasing

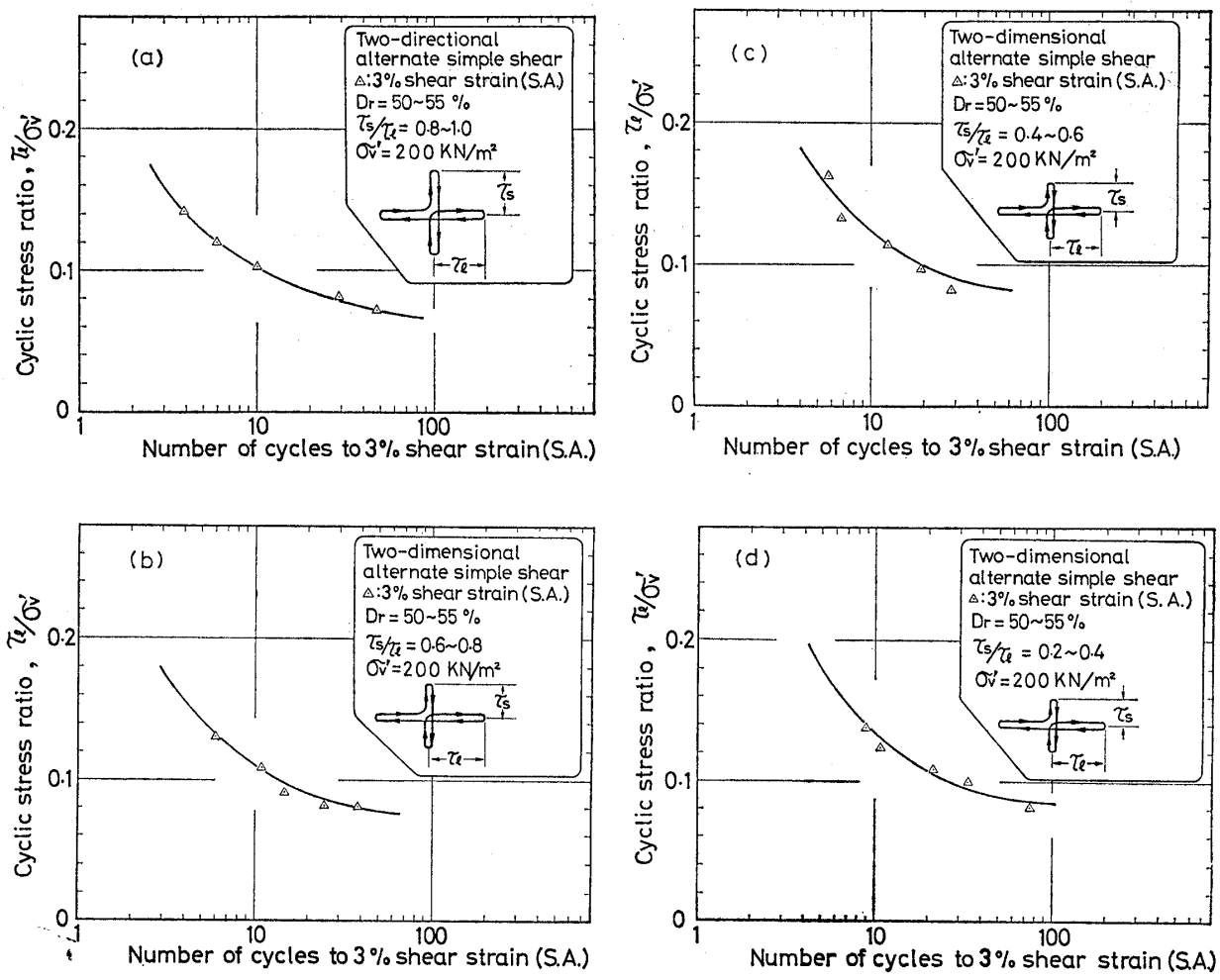

Fig. 15. Cyclic stress ratio versus number of cycles for alternate simple shear tests

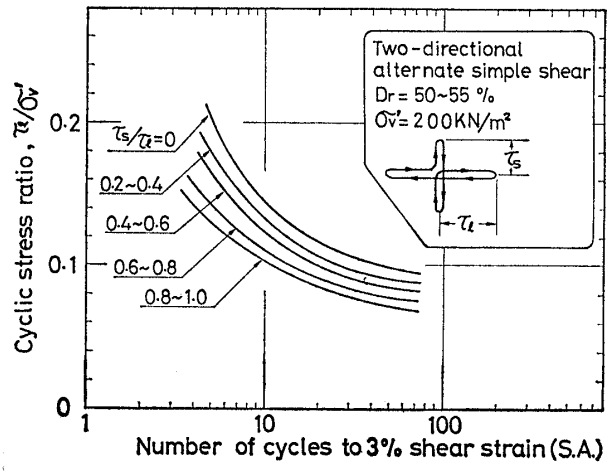

Fig. 16. Summary of the alternate simple shear test

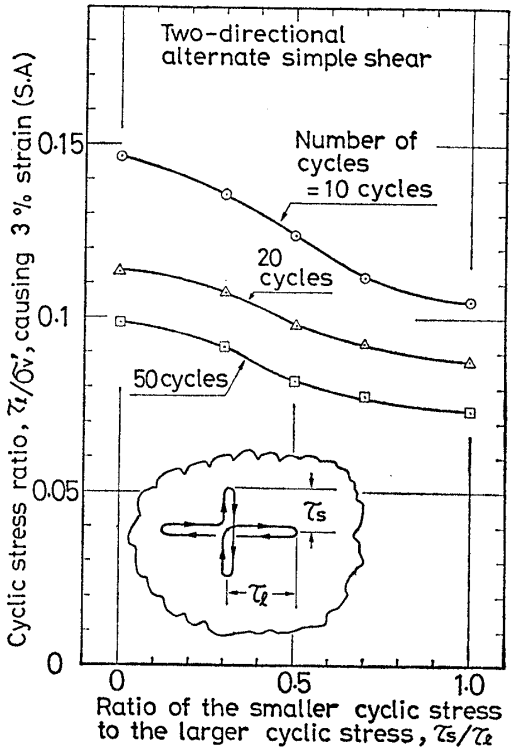

Fig. 17. Cyclic stress ratio versus cyclic stress amplitude ratio between two directions

stress amplitude in the direction perpendicular to the major loading direction was to decrease the cyclic stress ratio causing 3% failure strain in the direction of major loading. To see this effect more clearly, the cyclic stress ratio in the direction of larger shear stress application required to cause 3% single amplitude strain in 10, 20 and 50 cycles were read from Fig. 16 and replotted in Fig. 17 against the cyclic stress amplitude ratio, τ_s/τ_l. It may be seen in Fig. 17 that the cyclic strength in one direction of loading is reduced as the magnitude of cyclic stress in the other direction increased.

DISCUSSIONS OF THE TEST RESULTS

The results of the rotational simple shear tests summarized in Fig. 12 were arranged in such a way that it would be possible to visualize the effect of minor cyclic loading on the cyclic strength evaluated in terms of the cyclic stress ratio in the dircetion of major loading.

A most interesting interpretation is made possible by decomposing the rotational loading path into two components of shear stresses each acting independently in mutually perpendicular directions. In general, a rotational loading path may be regarded as a superposition of two sinusoidal loadings having an identical amplitude, τ_0, but having a phase lag, ψ, applied in mutually perpendicular directions in the horizontal simple shear plane. Denoting these two components by τ_x and τ_y, they are expressed as follows,

$$\left.\begin{aligned}\tau_x &= \tau_0 \sin(\omega t + \psi) \\ \tau_y &= \tau_0 \sin \omega t\end{aligned}\right\} \qquad (1)$$

where ω is angular frequency of cyclic loading and t denotes time. By eliminating the

parameter, ωt, between the two expressions in Eq. (1), one obtains the following equation.

$$\left(\frac{\tau_y}{\tau_0}\right)^2+\frac{1}{\sin^2\psi}\left(\frac{\tau_x}{\tau_0}-\frac{\tau_y}{\tau_0}\cos\psi\right)^2=1.0 \qquad (2)$$

This equation represents an elliptic curve with its long axis inclining 45° from τ_x-axis as shown in Fig. 18. To simplify Eq. (2), it will be desirable to perform a coordinate transformation by introducing another set of shear stresses, τ'_x and τ'_y, which are correlated with τ_x and τ_y as follows,

$$\left.\begin{aligned}\tau_x&=\tau'_x\cos 45°-\tau'_y\sin 45°\\ \tau_y&=\tau'_x\sin 45°-\tau'_y\cos 45°\end{aligned}\right\} \qquad (3)$$

By substituting Eq. (3) into Eq. (2), one obtains

$$\left(\frac{\tau'_x}{\tau_l}\right)^2+\left(\frac{\tau'_y}{\tau_s}\right)^2=1.0 \qquad (4)$$

where τ_l and τ_s are given by

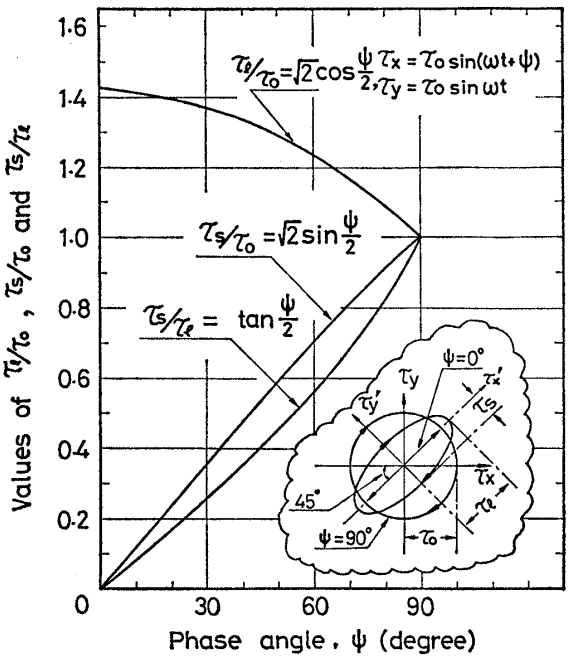

Fig. 18. Transformation between two stress coordinate systems

$$\left.\begin{aligned}\tau_l/\tau_0&=\sqrt{2}\cos\frac{\psi}{2}\\ \tau_s/\tau_0&=\sqrt{2}\sin\frac{\psi}{2}\end{aligned}\right\} \qquad (5)$$

It is obvious that τ_l and τ_s represent the longer and shorter axes of the ellipse in the new coordinate system, τ'_x and τ'_y as illustrated in Fig. 18. The value of τ_l/τ_0, τ_s/τ_0 and τ_s/τ_l as calculated from Eq. (5) as functions of the phase lag, ψ, are plotted in Fig. 18. From Eq. (5), it is possible to derive a formula correlating two cyclic stress ratios τ_0/σ'_v and τ_l/τ'_v with the value of τ_s/τ_l taken as a parameter,

$$\frac{\tau_0}{\sigma'_v}=\frac{\tau_l}{\sigma'_v}\sqrt{\frac{1}{2}+\frac{1}{2}\left(\frac{\tau_s}{\tau_l}\right)^2} \qquad (6)$$

In the rotational simple shear test described above, the ratio of the cyclic stress amplitude between X- and Y- directions was kept constant in each series of the test, that is, the ratio, τ_s/τ_l, was held approximately constant for each test result summarized in Fig. 12. Therefore, it may well be considered that the execution of the rotational simple shear test was made along the ellipic path whose coordinate axes were referred to τ'_x and τ'_y as illustrated Fig. 18. When the elliptic loading path thus expressed in the τ'_x and τ'_y coordinate system is transformed into the τ_x and τ_y coordinate system through Eq. (3), the elliptic loading path may be expressed in terms of superposition of two cyclic loadings executed in two mutually perpendicular direction. This transformation is equivalent to decomposing the rotational loading path into two components of loading as given by Eq. (1), in which τ_x and τ_y are expressed as functions of a common cyclic stress amplitude, τ_0, and a phase lag, ψ, between excursions of two cyclic loadings. The value of ψ can be determined readily from the curve in Fig. 18, when the cyclic stress amplitude ratio, τ_s/τ_l is known. The value of τ_0 can also be determined from the curves in Fig. 18, or by using Eq. (5).

The cyclic stress ratio, τ_l/σ'_v, with reference to the larger cyclic stress, required to cause

3% single amplitude simple shear strain in 10, 20 and 50 cycles, was plotted versus the cyclic stress amplitude ratio, τ_s/τ_l in Fig. 13. When the values of these two ratios, τ_l/σ'_v and τ_s/τ_l, corresponding to each data points are read off and used in Eqs. (5) and (6), it is possible to determine the values of the cyclic stress ratio, τ_0/σ'_v, and the phase lag, ψ. The cyclic stress ratio and the phase lag thus determined are plotted in Fig. 19. It may be seen in the figure that the cyclic stress ratio causing 3% single amplitude shear strain decreases with an increase in the phase lag up to the phase angle of approximately 45°, but the cyclic stress ratio remains nearly constant thereafter. It may also be noted that the effect of phase difference between the excursion of two cyclic loading becomes less as the number of cycles proceeds, where a smaller cyclic stress ratio is involved in causing 3% simple amplitude shear strain.

The common procedure for evaluating liquefaction resistance of sand has been to test the sand specimen in the laboratory using a cyclic triaxial or simple shear test apparatus in which loads are reciprocated only in one direction. In order to assess the cyclic strength in more realistic two-dimensional simple shear stress conditions with knowledge of the cyclic strength obtained from the conventional cyclic test, it will be desirable to provide a diagram in which the effect of the two-directional loading can clearly be visualized. For this purpose, the cyclic stress ratio causing 3% shear strain in 10, 20 and 50 cycles in the two-directional loading conditions was normalized to the corresponding cyclic stress ratio in the uni-directional loading condition by referring to the test data presented in Figs. 13 and 17. The result of normalization is shown in Fig. 20. It may be seen in the figure that the cyclic stress ratio causing 3% shear strain under rotational simple shear with two equal components are about 35% less than the similar cyclic stress ratio under uni-directional simple shear irrespective of the number of involved load cycles. The reduction in the cyclic stress ratio in the case of alternate simple shear from the cyclic stress ratio under one-directional simple shear is approximately 25%. Also indicated in Fig. 20 is the corresponding reduction in cyclic stress ratio under multi-directional loading condition reported by Seed, Pyke and Martin (1978). The reduction in cyclic stress ratio due to the presence

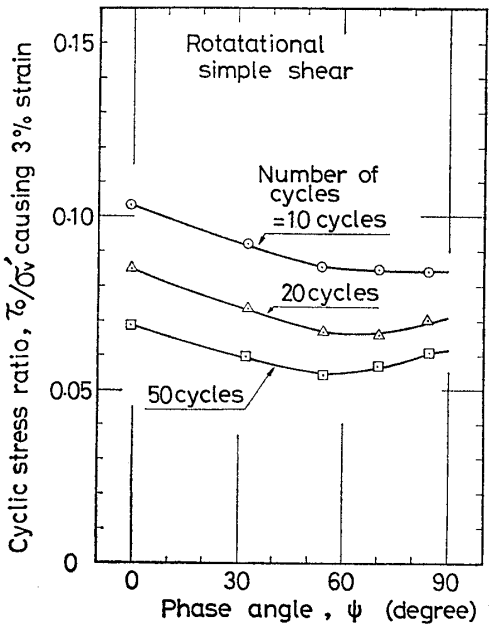

Fig. 19. Modified cyclic stress ratio versus phase lag angle between two loadings in two directions

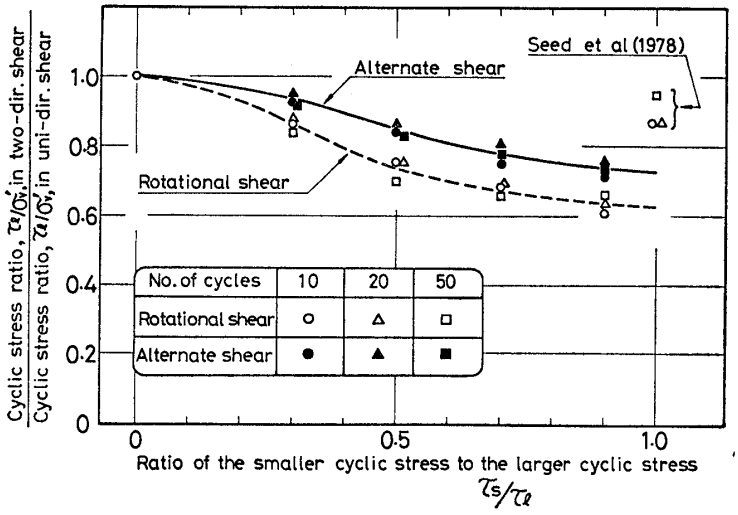

Fig. 20. Cyclic strength in the rotational and alternate simple shears normalized to the uni-directional simple shear

of a second component of equal amplitude is more pronounced in the result of the present study than in the shaking test result reported by Seed, Pyke and Martin (1978).

CONCLUSIONS

In the first series of multi-directional simple shear tests on loose saturated sand specimens employing circular and elliptic load paths with a phase difference of 90 degrees between two cyclic stresses in mutually perpendicular directions, it was shown that the cyclic stress ratio inducing 3% simple shear strain under a given number of cycles decreased as the amplitude of the second component was gradually increased, and when the second component grew as large as the main component the cyclic stress ratio dropped to approximately 65% of the cyclic stress ratio causing 3% strain under uni-directional loading condition. A similar decrease in cyclic stress ratio was also observed in the second series of multi-directional simple shear tests where two cyclic stresses in mutually perpendicular directions were alternately applied with a phase difference of 360 degrees. The maximum drop in the cyclic stress ratio of approximately 25% was attained in this test series as compared to the cyclic stress ratio in uni-directional loading when the amplitude of the second component became equal to that of the main component of simple shear motions.

ACKNOWLEDGEMENTS

The construction of the simple shear test apparatus was supported partly by the grant-in-aid for scientific research from the Ministry of Education. Performance of the simple shear tests was assisted by H. Yoshikane who worked towards his bachelor's degree on this test project. Dr. Kenji Mori kindly reviewed the draft of this paper. The writers wish to acknowledge the help offered by these agency and person.

REFERENCES

1) Casagrande, A. and Rendon, F. (1978) : "Gyratory shear apparatus design, testing procedures," Technical Report S-78-15, Corps of Engineer Waterways Experiment Station, Vicksburg Mississippi.
2) Ishihara, K., Iwamoto, S., Yasuda, S. and Takatsu, H. (1977) : "Liquefaction of anisotropically consolidated sand," Proc., 9 th International Conference on Soil Mechanics and Foundation Engineering, Vol. II, pp. 251-264.
3) Ishihara, K., Silver, M. L. and Kitagawa, H. (1978) : "Cyclic strengths of undisturbed sands obtained by large diameter sampling," Soils and Foundations, Vol. 18, No. 4, pp. 61-76.
4) Pyke, R. M., Seed, H. B. and Chan, C. K. (1975) : "Settlement of sands under multi-directional shaking," Proc., ASCE, GT 4, Vol. 101, pp. 370-398.
5) Seed, H. B., Pyke R. M. and Martin, G. R. (1978) : "Effect of multi-directional shaking on pore pressure development in sands," Proc., ASCE, GT 1, Vol. 104, pp. 27-44.

(Received April 9, 1979)